# CRYSTAL STRUCTURES AND CRYSTAL CHEMISTRY
## IN THE SYSTEM $Na_{1+x}Zr_2Si_xP_{3-x}O_{12}$*

H. Y-P. Hong
Lincoln Laboratory, Massachusetts Institute of Technology
Lexington, Massachusetts 02173

ABSTRACT

As part of a search for skeleton structures for fast alkali-ion transport, the system $Na_{1+x}Zr_2Si_xP_{3-x}O_{12}$ has been prepared, analyzed structurally and ion exchanged reversibly with $Li^+$, $Ag^+$, and $K^+$ ions. Single-crystal x-ray analysis was used to identify the composition $NaZr_2P_3O_{12}$ and to refine its structure, which has rhombohedral space group $R\bar{3}c$ with cell parameters $a_r = 8.815(1)Å$ and $c_r = 22.746(7)Å$. A small distortion to monoclinic symmetry occurs in the interval $1.8 \leq x \leq 2.2$. The structure for $Na_3Zr_2Si_2PO_{12}$, proposed from powder data, has space group $C2/c$ with $a_m = 15.586(9)Å$, $b_m = 9.029(4)Å$, $c_m = 9.205(5)Å$, and $\beta = 123.70(5)°$. Both structures contain a rigid, three-dimensional network of $PO_4$ or $(SiO_4)$ tetrahedra sharing corners with $ZrO_6$ octahedra and a three-dimensionally linked interstitial space. Of the two distinguishable alkali-ion sites in the rhombohedral structure, one is completely occupied in both end members, the occupancy of the other varies across the system from 0 to 100 percent. Several properties are compared with the fast $Na^+$-ion conductor $\beta$-alumina.

## Introduction

The research reported here was motivated by active interest in solid electrolytes having fast alkali-ion transport and by the proposition (1) that solid electrolytes having alkali-ion conductivities approaching those of liquids should occur in skeleton structures. Potential skeleton structures would consist of a rigid, three-dimensional network stabilized by electrons donated by transporting ions partially occupying a three-dimensionally linked interstitial space. Moreover, the smallest cross-sectional areas of an interstitial passageway, designated "bottlenecks" (2), should have smallest diameters greater than twice the sum of the anion and alkali-ion radii. For $Na^+$-ion transport in an oxide, the bottleneck smallest diameter should, therefore, exceed 4.8 Å.

In addition to these geometrical constraints, chemical bonding also plays a role. If the crystalline fields and/or the site binding energy preferentially stabilizes an alkali ion at a particular set of lattice sites, the activation energy for jumping

from one site to the next may be large even if the geometrical constraints of the bottlenecks are small. Creation of strong bonding within the rigid network should make the bonding between alkali ion and network more ionic and hence, perhaps, less site-specific if the geometrical constraints at the bottlenecks are not a problem. There are two ways that the strength of the intranetwork bonding can be increased relative to the bonding between alkali ion and network: (1) The anions can bond with more than two cations of the network and (2) the anions can form strongly covalent bonds with a cation to make a complex anion. In a three-dimensional network, each anion must bond with at least two cations of the network. If the anions bond to four or more network cations, the network is close-packed and there is no passageway for interstitial alkali ions. If anions bond to three network cations, layer structures such as $\beta$-alumina may be anticipated. The low activation energy of $\beta$-alumina may be at least partly due to the fact that all the oxygen atoms neighboring the alkali ions, except those in sites 2c of space group P6$_3$/mmc, are bonded by three aluminum atoms that polarize the $O^{2-}$-ion charge density away from the alkali ion. If the oxygen atoms bond to only two network cations, polarization of the $O^{2-}$-ion charge density away from the alkali ions is reduced, thus increasing the activation energy for ion transport according to our hypothesis. Since two-dimensional transport was not of interest in this study, geometry restricts each anion to bonding with at most two network cations. Therefore, it seemed appropriate to build the network with at least one cation that formed a strongly covalent complex, thus utilizing in effect a complex anion such as $SO_4^{2-}$, $NO_3^-$, $BO_3^{3-}$, $CO_3^{2-}$, $SiO_4^{4-}$, or $PO_4^{3-}$. A tetrahedral complex seemed a logical starting place. The companion cation of the network can have a tetrahedral-site preference or an octahedral-site preference. The Carnegieite structure of high-temperature $NaAlSiO_4$, for example, has tetrahedrally coordinated $Al^{3+}$ ions (1). In this work, the $Zr^{4+}$ ion was chosen because it is stable in octahedral coordination and because zirconium oxides are not reduced by molten sodium.

This paper reports the synthesis and structural characterization of compounds in the system $Na_{1+x}Zr_2Si_xP_{3-x}O_{12}$, $0 \leq x \leq 3$, all of which can be reversibly ion-exchanged with $Li^+$, $Ag^+$, and $K^+$ ions in molten salts. The relationship of this work to a comprehensive investigation of skeleton structures is discussed in a companion paper (1), where preliminary transport measurements are also presented.

## Experimental Procedure

The starting materials $Na_2CO_3$, $ZrO_2$ and $NH_4H_2PO_4$ were mixed in the Na-Zr-$PO_4$ ratios 212, 513, 123, 725, 547, and 759. The mixtures were preheated at 170° for 4 hours to decompose the $NH_4H_2PO_4$, at 900°C for 4 hours to decompose the $Na_2CO_3$, and overnight at 1200°C to transform any metaphosphate to orthophosphate. Normally, a metaphosphate decomposes to orthophosphate above about 1000°C (3). With the exception of mixes 513 and 725, the x-ray data of all products showed a single crystalline phase, as listed in Table 1. Interestingly, the mixes 212, 547, and 759 gave identical x-ray powder patterns having a somewhat smaller unit cell than that of mix 123. To obtain a single crystal of this dominant phase, a 212 mix was heated for 3 hours at 1600°C before the furnace was turned off. The crystals obtained for x-ray analysis by this procedure were typically cube-shaped, about 0.1 mm on a side. From the structure determination, the chemical composition was found to be $NaZr_2P_3O_{12}$. The structure consisted of an open network of $(PO_4)^{3-}$ tetrahedra coordinated octahedrally to $Zr^{4+}$ ions with $Na^+$ ions filling a unique set of sites in a three-dimensionally linked interstitial space. The substitution of $P^{5+}$ ions by ($Si^{4+}$ + $Na^+$) ions was attempted to introduce $Na^+$ ions into other positions of the interstitial space, an appropriate preparation of $SiO_2$ being added to the starting mix. Complete solid solution was found for the system $Na_{1+x}Zr_2Si_x$ $P_{3-x}O_{12}$, $0 \leq x \leq 3$. Indeed, the end member $Na_4Zr_2Si_3O_{12}$ has previously been reported (4). X-ray data for compounds in this system are listed in Table 1. All structures were rhombohedral R$\bar{3}$c except in the range $1.8 \leq x \leq 2.2$, where a distortion to monoclinic C2/c symmetry occurs. The structure of $NaZr_2P_3O_{12}$ was

## TABLE 1

X-ray Data for Compounds in the System $Na_{1+x}Zr_2Si_xP_{3-x}O_{12}$

| Starting Composition | Space Group | a | b | c | β | V |
|---|---|---|---|---|---|---|
| $Na_2Zr(PO_4)_2$ | $R\bar{3}c$ | 8.792(5) | | 22.723(9) | | 1521.0 |
| $Na_5Zr_4(PO_4)_7$ | $R\bar{3}c$ | 8.794(5) | | 22.721(9) | | 1522.7 |
| $Na_7Zr_5(PO_4)_9$ | $R\bar{3}c$ | 8.795(5) | | 22.722(9) | | 1523.2 |
| $NaZr_2(PO_4)_3$ | $R\bar{3}c$ | 8.815(1) | | 22.746(7) | | 1530.5 |
| $Na_{1.4}Zr_2Si_{0.4}P_{2.6}O_{12}$ | $R\bar{3}c$ | 8.840(3) | | 22.731(9) | | 1538.3 |
| $Na_{1.8}Zr_2Si_{0.8}P_{2.2}O_{12}$ | $R\bar{3}c$ | 8.898(1) | | 22.774(8) | | 1561.6 |
| $Na_{2.2}Zr_2Si_{1.2}P_{1.8}O_{12}$ | $R\bar{3}c$ | 8.940(3) | | 22.855(9) | | 1581.9 |
| $Na_{2.6}Zr_2Si_{1.6}P_{1.4}O_{12}$ | $R\bar{3}c$ | 8.980(5) | | 22.906(9) | | 1599.6 |
| $Na_{2.8}Zr_2Si_{1.8}P_{1.2}O_{12}$ | C 2/c | 15.567(9) | 9.003(5) | 9.217(6) | 123.76(5) | $1610.8 \times \frac{2}{3}$ |
| $Na_{3.0}Zr_2Si_2PO_{12}$ | C 2/c | 15.586(9) | 9.029(4) | 9.205(5) | 123.70(5) | $1616.6 \times \frac{2}{3}$ |
| $Na_{3.2}Zr_2Si_{2.2}P_{0.8}O_{12}$ | C 2/c | 15.618(9) | 9.051(6) | 9.210(9) | 123.93(6) | $1620.6 \times \frac{2}{3}$ |
| $Na_{3.4}Zr_2Si_{2.4}P_{0.6}O_{12}$ | $R\bar{3}c$ | 9.079(2) | | 22.685(9) | | 1619.3 |
| $Na_{3.8}Zr_2Si_{2.8}P_{0.2}O_{12}$ | $R\bar{3}c$ | 9.148(4) | | 22.239(9) | | 1611.6 |
| $Na_4Zr_2Si_3O_{12}^*$ | $R\bar{3}c$ | 9.10 | | 22.07 | | 1583.9 |

[*]Ref. 4



FIG. 1

Projection of half the unit cell along the $a_r$-axis of rhombohedral $NaZr_2^rP_3O_{12}$
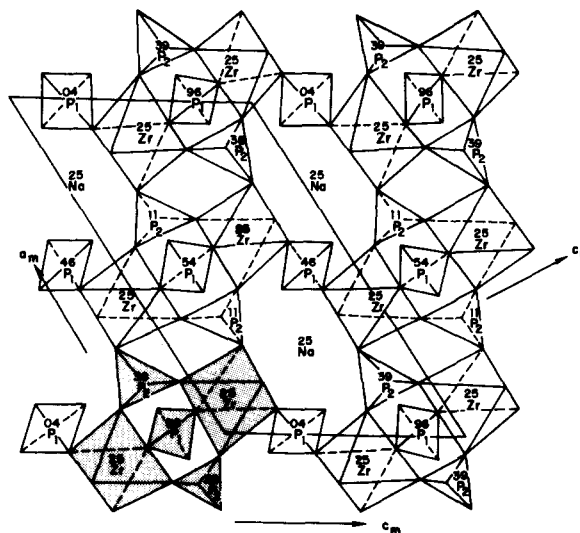
refined by single-crystal x-ray analysis. Attempts to grow single-crystal $Na_3Zr_2Si_2PO_{12}$ failed, but the distortion of the network is small enough that the network configuration in monoclinic $Na_3Zr_2Si_2PO_{12}$ could be deduced from powder data. Without single-crystal data, it is not possible to say anything definitive about the $Na^+$-ion distribution. However, there are $Na_2$ and $Na_3$ positions in addition to the $Na_1$ positions in the interstitial space that can accommodate the extra sodium.

An interesting feature of Table 1 is that the unit-cell size does not increase monotonically with x, as might be anticipated for a $Si^{4+}$ radius of 0.40 Å vs a $P^{5+}$ radius of only 0.31 Å. Rather, it reaches a maximum near x = 2.2, and the monoclinic C2/c phase is associated with the compositions having the largest rhombohedral $c_r$-axis, which produces the largest unit-cell volume.

## Structure of $NaZr_2P_3O_{12}$

A cube-shaped crystal about 0.05 mm on an edge was selected for x-ray-diffraction analysis. Oscillation and Weissenberg photographs showed diffraction symmetry $\bar{3}m$. The systematic absences were hkℓ, -h + k + ℓ = 3n + 1, and h0ℓ with ℓ = 2n + 1, which is consistent with space groups R3c and R̄3c. Three-dimensional intensity data to 2θ = 50° were collected with Mo radiation as described elsewhere (5). In total, 705 reflections were measured. The heavy-atom method was used to solve the structure.

The true composition of the crystal was initially unknown. A strong peak at (0,0,0.29) in the Patterson map was assumed to represent an interaction between the Zr atoms. Therefore, twelve Zr atoms were assigned to the 12e positions at (0.0,0.145). From a Patterson map peak at (0,0,0.145), the Na atoms were assigned to the 6b positions at (0,0,0). A structure-factor calculation based on these positions gave a difference-function R value of 0.35. With this model and the assumption of R̄3c symmetry, it was possible to identify from a difference Fourier synthesis one P atom and two O atoms. The atom parameters, scale factors, and anisotropic temperature factors were then refined with a full-matrix, least-squares program to give R = 0.043 and $R_w$ = 0.060 for all reflections. The final values are listed in Table 2. Subsequently it was learned that Hagman and Kierkegaard (6) had reported the structure of $NaZr_2P_3O_{12}$. With the same space group, they obtained an R = 0.089. Their atomic parameters are listed in parentheses in Table 2. Both analyses gave high isotropic temperature factors for the $Na^+$ ions, indicating that these ions are mobile. In the present study, anisotropic temperature factors were refined. They show high mobility along the $a_r$ axes, which are parallel to the tunnels of the interstitial space.

TABLE 2

Final Atomic Parameters for $NaZr_2P_3O_{12}$ (Numbers in parentheses from Ref. 6)

Space group R̄3c; cell parameter a = 8.815(1) Å, c = 22.746(7) Å

|  | x | y | z | $\beta_{11}$ | $\beta_{22}$ | $\beta_{33}$ | $\beta_{12}$ | $\beta_{13}$ | $\beta_{23}$ | $\beta_0$ |
|---|---|---|---|---|---|---|---|---|---|---|
| Na | 0 | 0 | 0 | 0.036(2) | 0.022(1) | 0.0010(2) | 1/2 $\beta_{11}$ | 0 | 0 | 4.0(2) (4.2±2) |
| Zr | 0 | 0 | 0.14568(6) (0.1456 ± 1) | 0.0036(2) | 0.0036(2) | 0.00023(3) | 1/2 $\beta_{11}$ | 0 | 0 | 0.78(4) (1.80±7) |
| P | 0.2916(3) (0.2909 ± 6) | 0 | 1/4 | 0.002(1) | 0.0054(7) | 0.00055(7) | 1/2 $\beta_{11}$ | 0.0002(3) | 1/2 $\beta_{23}$ | 1.08(7) (2.4±1) |
| O(1) | 0.1841(7) (0.1860 ± 15) | -0.0165(7) (-0.0144 ± 15) | 0.1956(2) (0.1949 ± 5) | 0.006(1) | 0.008(1) | 0.0006(1) | 0.005(1) | 0.006(3) | 0.0001(3) | 1.4(1) (3.2±2) |
| O(2) | 0.1911(8) (0.1913 ± 15) | 0.1675(8) (0.1683 ± 15) | 0.0876(2) (0.0866 ± 5) | 0.007(1) | 0.005(1) | 0.0006(1) | 0.003(1) | 0.0004(3) | 0.0000(3) | 1.5(1) (2.9±2) |

The structure consists of a three-dimensional skeletal network of $PO_4$ tetrahedra corner-sharing with $ZrO_6$ octahedra, the $Na^+$ ions occupying a large octahedral site in the interstitial space. Each $ZrO_6$ octahedra is connected to six $PO_4$ tetrahedra, while each tetrahedra is linked to four octahedra. A projection along the $c_r$-axis can be found in Ref. 6. The projection of half the unit cell along the $a_r$-axis, which permits visualization of the empty interstitial space inside the network, is shown in Fig. 1. The rhombohedral cell can also be indexed as a monoclinic cell with $a_m = 2a_r \sin 60° = 15,268$ Å, $b_m = a_r = 8.815$ Å, $c_m = c_r/3 \cos (\beta-90) = 9.130$ Å, and $\beta = 123.85°$. The basic unit of the network, which is shaded in Fig. 1, consists of two octahedra joined by three tetrahedra, corresponding to $(Zr_2P_3O_{12})^-$. These units are connected so as to form a ribbon along the $[100]_m$ direction, and the ribbons are linked together by $P(1)O_4$ tetrahedra to form a two-dimensional sheet. The second half of the unit cell is a similar sheet with Zr atoms at $b_m = 0.75$ instead of $b_m = 0.25$ and displaced $c_m/2$, as indicated in Fig. 2. The Na atoms are located at $Na_1$ sites in $NaZr_2P_3O_{12}$. A $Na_1(25)$ is octahedrally coordinated by $O^{2-}$ ions of the two neighboring $Zr(25)O_6$ octahedra. It is also octahedrally coordinated by $6Na_2$(rhomb) = 2 $Na_2$(mono) + 4 $Na_3$(mono) sites located in the same rhombohedral basal plane as the nearest-neighbor oxygen atoms. The bottleneck in the passageway from a $Na_1$ site to a $Na_2$ or $Na_3$ site is a puckered hexagonal ring having sides that alternate between octahedral and tetrahedral edges. The shortest diameter of the bottleneck is larger than 4.8 Å, twice the sum of $Na^+$-ion and $O^{2-}$-ion radii. Thus the geometrical features of the skeleton and its interstitial space satsify the criteria for fast $Na^+$-ion transport, provided the site-preference energy for a $Na_1$ position is not too much greater than those for $Na_2$ or $Na_3$ positions.

## Proposed Structure of $Na_3Zr_2Si_2PO_{12}$

As indicated in Table 1, the x-ray powder pattern of $Na_3Zr_2Si_2PO_{12}$ can only be indexed on a monoclinic cell. In the absence of single crystals, the single-

### TABLE 3

Final Atomic Parameters for $NaZr_2P_3O_{12}$ and Proposed $Na_3Zr_2Si_2PO_{12}$

Space group C2/c; cell parameters for $NaZr_2P_3O_{12}$: $a_m = 15.266(3)$ Å, $b_m = 8.815(2)$ Å, $c_m = 9.130(1)$ Å, $\beta = 123.83(3)°$

cell parameters for $Na_3Zr_2Si_2PO_{12}$: $a_m = 15.586(9)$ Å, $b_m = 9.029(4)$ Å, $c_m = 9.205(5)$ Å, $\beta = 123.70(5)°$

| | x | y | z | $\beta_{11}$ | $\beta_{22}$ | $\beta_{33}$ | $\beta_{12}$ | $\beta_{13}$ | $\beta_{23}$ | $\beta_0$ |
|---|---|---|---|---|---|---|---|---|---|---|
| Na(1) | 1/4 | 1/4 | 1/2 | 0.006(1) | 0.017(2) | 0.004(3) | 0 | 0 | 0 | 3.8(2) |
| Zr | 0.1043(1) | 0.2498(2) | 0.0629(2) | 0.0009(1) | 0.0019(2) | 0.0015(2) | 0.0000(1) | 0.0002(1) | 0.0000(1) | 0.62(4) |
| P(1) | 0 | 0.0412(8) | 1/4 | 0.0017(5) | 0.002(1) | 0.004(1) | 0 | 0.0016(7) | 0 | 0.9(1) |
| P(2) | 0.354(3) | 0.1051(6) | 0.2493(6) | 0.0015(3) | 0.0022(8) | 0.004(1) | 0.0000(3) | 0.0011(5) | 0.0000(8) | 0.9(1) |
| O(1) | 0.149(1) | 0.43(1) | 0.234(1) | 0.003(1) | 0.000(2) | 0.004(2) | 0.000(1) | 0.001(1) | 0.001(2) | 1.2(2) |
| O(2) | 0.438(1) | 0.44(1) | 0.088(1) | 0.002(1) | 0.004(2) | 0.004(3) | 0.000(1) | 0.000(1) | 0.001(2) | 1.4(2) |
| O(3) | 0.259(1) | 0.172(1) | 0.237(1) | 0.0013(9) | 0.003(2) | 0.004(2) | 0.000(1) | 0.001(1) | 0.003(2) | 1.0(2) |
| O(4) | 0.353(1) | 0.144(1) | 0.085(1) | 0.003(1) | 0.005(2) | 0.004(3) | 0.001(1) | 0.002(1) | 0.000(2) | 1.4(2) |
| O(5) | 0.453(1) | 0.169(1) | 0.412(1) | 0.001(1) | 0.005(2) | 0.008(3) | 0.002(1) | 0.000(1) | 0.000(2) | 1.6(2) |
| O(6) | 0.078(1) | 0.139(1) | 0.240(1) | 0.0014(9) | 0.001(2) | 0.005(2) | 0.000(1) | 0.002(1) | 0.002(2) | 0.9(2) |
| Na(2) | 0.50 | 0.95 | 1/4 | | | | | | | |
| Na(3) | 0.83 | 0.10 | 0.70 | | | | | | | |

crystal intensity data of $NaZr_2P_3O_{12}$ were reindexed on a monoclinic cell with $h_m = h_r - k_r$, $k_m = h_r + k_r$, and $\ell_m = (\ell_r - h_r + k_r)/3$. The positions of all atoms of single-crystal $NaZr_2P_3O_{12}$ were located from calculation of the Patterson map and, subsequently, of the difference Fourier map. The least squares refinement based on this new monoclinic space group C2/c gave the final atomic parameters listed in Table 3. An abnormally large isotropic temperature factor indicative of large thermal motion was observed along the $b_m$-axis, the only monoclinic axis parallel to a passageway between sodium sites ($Na_1$ and $Na_3$).

The proposed structure for $Na_3Zr_2Si_2PO_{12}$ is based on the following three assumptions: (1) the Si atoms are ordered in the P(2) positions, (2) the excess Na atoms are randomly distributed over positions 4e (0.50, 0.95, 0.25) and 8f(0.83, 0.10, 0.70), the $Na_2$ and $Na_3$ positions in Fig. 2, but electrostatic $Na^+$-$Na^+$ interactions and thermal motion make all the Na sites average positions with a large Debye-Waller factor, and (3) the network, though distorted and enlarged relative to $NaZrP_3O_{12}$, remains intact. The large, polyhedral sites $Na_2$ and $Na_3$ have Na-O distances greater than 2.4 Å, the sum of the $Na^+$ and $O^{2-}$ ionic radii. Table 4 lists the bond distances calculated from powder data based on this proposed structure. The hexagonal bottlenecks between $Na_1$ and $Na_2$ or $Na_3$ positions are formed, as shown in Fig. 3, by three $ZrO_6$ octahedral edges alternating with three tetrahedral edges, one $PO_4$ and two $SiO_4$. The shortest diameter across this hexagon is 4.95 Å, which is larger than twice the sum of the $Na^+$ and $O^{2-}$ ionic radii 4.8 Å. Each $Na_2$ or $Na_3$ site is connected through a bottleneck to two $Na_1$ sites, but there is no passageway between $Na_2$ sites or a $Na_2$ and a $Na_3$ site. The six channels through each $Na_1$ site provide a three-dimensionally linked interstitial space.

## Ion Exchange of $NaZr_2P_3O_{12}$ and $Na_3Zr_2Si_2PO_{12}$

Characteristically, three-dimensional ionic conductors exchange alkali ions with a molten salt bath, the chemical concentration gradient acting as the driving

## TABLE 4

Bond Distances (Å) in Proposed Structure of $Na_3Zr_2Si_2PO_{12}$

| Polyhedron around Na(1) | | Polyhedron around Na(2) | | Polyhedron around Na(3) | |
|---|---|---|---|---|---|
| Na(1)-O(1) | 2 x 2.620 | Na(2)-O(1) | 2 x 2.413 | Na(3)-O(1) | 3.019 |
| Na(1)-O(3) | 2 x 2.599 | Na(2)-O(4) | 2 x 2.600 | Na(3)-O(2) | 3.031 |
| Na(1)-O(6) | 2 x 2.608 | Na(2)-O(5) | 2 x 2.808 | Na(3)-O(2) | 2.441 |
| Na(1)-Na(2) | 2 x 3.713 | Na(2)-O(5) | 2 x 2.974 | Na(3)-O(3) | 3.031 |
| Na(1)-Na(3) | 2 x 3.519 | Na(2)-O(6) | 2 x 3.081 | Na(3)-O(3) | 2.449 |
| Na(1)-Na(3) | 2 x 3.852 | Na(2)-Na(1) | 2 x 3.713 | Na(3)-O(4) | 2.621 |
| | | | | Na(3)-O(4) | 2.648 |
| Octahedron around Zr | | Tetrahedron around P | | Na(3)-O(5) | 2.772 |
| Zr-O(1) | 2.104 | PO-O(2) | 2 x 1.542 | Na(3)-O(6) | 2.478 |
| Zr-O(2) | 2.077 | PO-O(6) | 2 x 1.546 | Na(3)-Na(1) | 3.519 |
| Zr-O(3) | 2.142 | | | Na(3)-Na(1) | 3.852 |
| Zr-O(4) | 2.055 | Tetrahedron around Si | | Na(3)-Na(3) | 4.114 |
| Zr-O(5) | 2.096 | Si-O(1) | 1.583 | | |
| Zr-O(6) | 2.137 | Si-O(3) | 1.545 | | |
| | | Si-O(4) | 1.543 | | |
| | | Si-O(5) | 1.546 | | |

force. Accordingly, powders of $NaZr_2P_3O_{12}$ and $Na_3Zr_2Si_2PO_{12}$ were held for four hours in molten $LiNO_3$, $AgNO_3$, and $KNO_3$, respectively. The powder:salt weight ratio was 1:20. The products were washed with water to remove the nitrates, dried, and analyzed by x-ray powder diffraction. The ion-exchanged cell parameters are listed in Table 5.
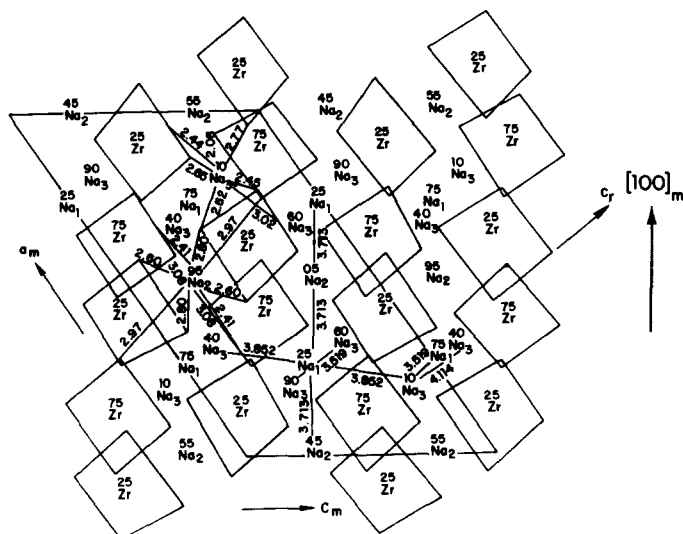


FIG. 2

Projection along the $b_m$-axis of the proposed monoclinic cell of $Na_3Zr_2Si_2PO_{12}$. Each Na(1) site is channeled three-dimensionally to two Na(2) sites and four Na(3) sites, and each Na(2) site or Na(3) site is linked to two Na(1) sites.
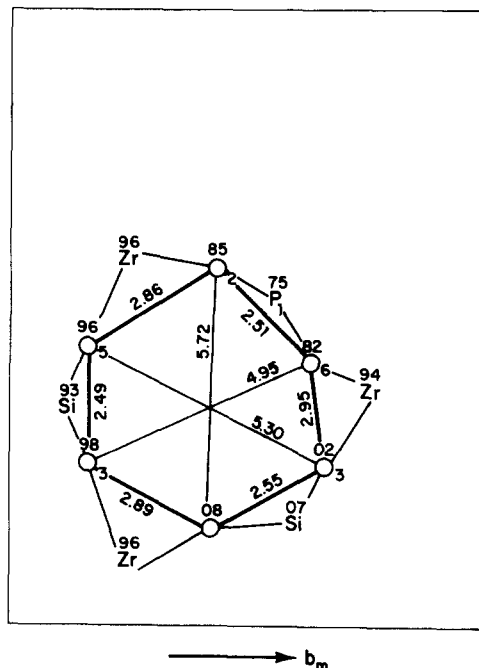


FIG. 3

A "bottleneck" of $Na_3Zr_2Si_2PO_{12}$ formed by three $ZrO_6$-octahedral edges and three (two $SiO_4$ and one $PO_4$) tetrahedral edges with a shortest diameter of 4.95 Å.

Replacement of the $Na^+$ ions by $Li^+$ ions in $NaZr_2P_3O_{12}$ tests the rigidity of the $(Zr_2P_3O_{12})^-$ network. Because the $Li^+$ ion is considerably smaller than the $Na^+$ ion, the network would be expected to collapse were it bonded tightly to the alkali ion. In fact, the network does not collapse. There is only a decrease in the unit-cell volume. Interestingly, the systematic increase in cell volume for $MZr_2P_3O_{12}$ on going from M = Li to Na to Ag to K in Table 5 is due to an increase in $c_r$, the parameter $a_r$ actually decreasing slightly. From Fig. 1, the alkali ion occupies an $M_1$ position, which has as nearest neighbors two octahedral-site faces on opposite sides parallel to the basal plane. Clearly the spacing between these octahedral-site faces, and hence the size of $c_r$, will vary sensitively with the size of the $M_1^+$ cation. A tensile stretch along the $c_r$-axis is accompanied by a contraction in the basal plane. In $NaZr_2P_3O_{12}$, the $Na_1$-O distance is 2.6 Å, smaller than the sum of $K^+$ and $O^{2-}$ ionic radii (2.75 Å), so an expansion of $c_r$ must occur in $KZr_2P_3O_{12}$.

The situation is more complex for the series $M_3Zr_2Si_2PO_{12}$, where M = Li, Ag, and K. In the first place, only if M = Na is the space group monoclinic C2/c. In the second place, the $c_r$-axis for M = $Li^+$ is anomalously large, even though the cell volume is small, which indicates that the $Li^+$ ions occupy different positions in the interstitial space. The most probable position would be at a bottleneck, since this would allow the shortest Li-O distances. Such a conjecture is supported by the anomalous variation with x of the lattice parameters for the system $Na_{1+x}Zr_2Si_x$

## TABLE 5

X-ray Data for Ion-exchanged $NaZr_2P_3O_{12}$ and $Na_3Zr_2Si_2PO_{12}$

| Compound | Space Group | a($\mathring{A}$) | b($\mathring{A}$) | c($\mathring{A}$) | $\beta(°)$ | V($\mathring{A}$)$^3$ |
|---|---|---|---|---|---|---|
| $LiZr_2P_3O_{12}$ | $R\bar{3}c$ | 8.817(5) | | 22.561(9) | | 1518.8 |
| $NaZr_2P_3O_{12}$ | $R\bar{3}c$ | 8.815(1) | | 22.746(7) | | 1530.5 |
| $AgZr_2P_3O_{12}$ | $R\bar{3}c$ | 8.814(1) | | 22.889(7) | | 1539.8 |
| $KZr_2P_3O_{12}$ | $R\bar{3}c$ | 8.710(1) | | 23.841(9) | | 1566.5 |
| $Li_3Zr_2Si_2PO_{12}$ | $R\bar{3}c$ | 8.554(5) | | 23.314(9) | | 1477.4 |
| $Na_3Zr_2Si_2PO_{12}$ | C 2/c | 15.586(9) (9.029) | 9.029(4) | 9.205(5) (22.974) | 123.70(5) | 1616×2/3 |
| $Ag_3Zr_2Si_2PO_{12}$ | $R\bar{3}c$ | 9.058(3) | | 23.059(9) | | 1638.5 |
| $K_3Zr_2Si_2PO_{12}$ | $R\bar{3}c$ | 8.940(3) | | 23.721(9) | | 1641.8 |

$P_{3-x}O_{12}$ given in Table 1. The fact that "$c_r$" is a maximum near $x = 2.2$ is compatible with electrostatic repulsions between $Na^+$ ions forcing displacement toward the bottleneck positions, thus contributing to the large Debye-Waller factor. Hybridization of the $4d^{10}$ core orbitals with empty 5s and 5p orbitals at a $Ag^+$ ion would permit it to accommodate to a bottleneck position (7), and it appears from Table 5 that the $Ag^+$-ion distribution is similar to the $Na^+$-ion distribution. The larger $K^+$ ions, on the other hand, would not be so easily accommodated in the bottleneck positions, and smaller $K^+$-ion displacements are compatible with Table 5.

Because the energy of hybridization at a $Ag^+$ ion is comparable to the increased covalent-bond energy made possible in oxides by hybridization, the Ag-O bond length may vary over quite a range from compound to compound. Shorter bond lengths signal hybridization and a stronger covalent component, which results in turn in a darkening of the crystal (7). If a silver oxide is white, the Ag-O distance is longer than 2.4 $\mathring{A}$ and the bond is largely ionic. As the Ag-O distance shortens, the color of the silver oxide changes from white to yellow to orange to brown to black. Therefore, if ion-exchange with $Ag^+$ ions produces a dark product, two inferences can be made: (1) the intranetwork bonding is not strong enough to inhibit hybridization at the $Ag^+$ ion with formation of a strong covalent contribution to the Ag-O bond and (2) it may not be possible to reverse ion-exchange from $Ag^+$ to $Na^+$ because of the tight Ag-O bond. In such a case, the Na-O bonding is expected to be strong enough to make the activation energy for $Na^+$-ion transport relatively larger. The $AgZr_2P_3O_{12}$ obtained from ion-exchanged $NaZr_2P_3O_{12}$ in molten $AgNO_3$ is white, indicating ionic Ag-O bonding and strong intranetwork bonding. This observation is consistent with the lattice-parameter variations of Table 5. The color of $Ag_3Zr_2Si_2PO_{12}$, on the other hand, is light yellow, indicating that at least some of the $Ag^+$ ions have an appreciable covalent contribution to some Ag-O bonds. Such would be the case were some $Ag^+$ ions displayed toward the bottleneck positions. The fact that the Ag compound can be reverse ion-exchanged indicates that the covalent contribution to the Ag-O bond is not too strong.

The fact that the compounds can be reverse ion-exchanged with $K^+$ ions

shows that the bottlenecks are large enough to permit the large $K^+$ ions to pass. Therefore, we anticipate fast $Na^+$-ion conduction in the system $Na_{1+x}Zr_2Si_xP_{3-x}O_{12}$.

## Discussion

The system $Na_{1+x}Zr_2Si_xP_{3-x}O_{12}$ has a skeleton structure consisting of a rigid, three-dimensional network stabilized by electrons from mobile alkali ions in a three-dimensionally linked interstitial space. As such, it is one of a class of compounds showing promise for fast ion conduction (1). In general, such structures are plagued by the fact that the interstitial space may accept, in addition to the alkali ions of interest, small molecules like $H_2O$ or $Na_2O$ that block alkali-ion transport (1). Indeed, this problem is also common to β-alumina (8). The system under study here does not become hydrated, but there is some evidence that excess $Na_2O$ may be incorporated. The cell parameters obtained from the original 212, 547, and 759 mixes, which contained an excess of $Na_2O$, were different (see Table 1) from those of the single crystal, which was grown from a 212 mix fired for a few hours at a high enough temperature (1600 °C) to drive off excess $Na_2O$. The single-crystal data gave no evidence of excess $Na_2O$.

In $NaZr_2P_3O_{12}$, the $Na_1$ positions are filled and the $Na_2$ positions are empty. Since the site-preference energies for the two positions are not equal, the activation energy for $Na^+$-ion conduction may be large. In the system $Na_{1+x}Zr_2Si_x P_{3-x}O_{12}$, on the other hand, the introduction of excess $Na^+$ ions introduces electrostatic $Na^+$-$Na^+$ interactions that can lower the activation energy even though transport must be via a $Na_1$ site. The structural evidence for displacement of $Na^+$ ions toward bottleneck positions in $Na_3Zr_2Si_2PO_{12}$ indicates that this is the case, and indeed the transport properties at 300°C are comparable to those of the best β″-alumina (1).

In closing, it is interesting to compare the properties of $Na_3Zr_2Si_2PO_{12}$ investigated here with those of β-alumina.

(1) In both compounds, the $Na^+$ ions can be exchanged reversibly in molten salts with $Li^+$, $Ag^+$, and $K^+$ ions.

(2) In both compounds, the lattice parameters of the $Li^+$-exchanged products indicate that the $Li^+$ ions occupy different lattice positions than the $Na^+$ ions.

(3) In both compounds, available alkali-ion positions are crystallographically inequivalent, and the total number of positions is only partially occupied.

(4) In $Na_3Zr_2Si_2PO_{12}$ the bottleneck to $M^+$-ion transport is a hexagon with a shortest Na-O contact of 2.475 Å; in β-alumina it is a rectangle between sites 2b and 2d of $P6_3/mmc$ with a shortest Na-O contact of 2.71 Å, and the 2b position itself is a midpoint between two $O^{2-}$ ions separated by 4.84 Å.

(5) In β-alumina, the $Na^+$ ions are constrained to two-dimensional motion; in $Na_3Zr_2Si_2PO_{12}$ they move in three dimensions and the Na-site density is twice as large: 11.13 vs 5.57 $\times 10^{21}$ $cm^{-3}$.

(6) Whereas β-alumina has an anisotropic thermal expansion, pseudocubic $Na_3Zr_2Si_2PO_{12}$ may have a nearly isotropic thermal expansion, thus minimizing thermally induced stresses at grain boundaries of a ceramic membrane.

(7) Both compounds are stable in molten sodium.

(8) Ceramic processing of $Na_3Zr_2Si_2PO_{12}$ can be achieved at around 1200°C, substantially below the 1500°C needed for β-alumina.

## References

1. J. B. Goodenough, H. Y-P. Hong, and J. A. Kafalas, Companion Paper.

2. H. Y-P. Hong, Acta. Cryst. B30, 945 (1974).

3. H. Y-P. Hong, Mat. Res. Bull. 10, 635 (1975).

4. R. G. Sizova, A. A. Voronkov, N. G. Shumyatskaya, V. V. Pyakhim, and N. V. Belov, Dokl. Akad. Nank SSSR, Ser. 205, Issue 1, 90 (1972).

5. H. Y-P. Hong, Acta. Cryst. B30, 468 (1974).

6. L. Hagman and P. Kierkegaard, Acta. Chem. Scan. 22, 1822 (1968).

7. H. Y-P. Hong, J. A. Kafalas, and J. B. Goodenough, J. Sol. State Chem. 9, 345 (1974).

8. W. L. Roth, W. C. Hamilton, and S. J. Laplace, Am. Cryst. Assoc. Abstr., Ser. 2, 1, 169 (1973).